Chemical Engineering Journal 101 (2004) 339–345

Chemical Engineering Journal

www.elsevier.com/locate/cej

Characterisation of electrically powered micro-heat exchangers☆

Torsten Henning*, Juergen J. Brandner, Klaus Schubert

Forschungszentrum Karlsruhe, Institute for Micro Process Engineering IMVT, P.O. Box 3640, DE-76021 Karlsruhe, Germany

Received 30 July 2003; accepted 28 October 2003

Abstract

Electrically powered micro-heat exchangers built from foils containing microchannels and from spacer blocks with electrical heater cartridges were compared for water throughputs of up to 64 kg/h and for electrical powers up to 3 kW. A reference design and two variations of this design were characterised with regard to their power conversion efficiency, and to the correlation between the maximum heater cartridge temperature and the outlet temperature. The design variation with shortened microchannels showed improved thermal conversion for flow rates around 2 kg/h. The other design variation, replacing straight microchannels with curved meanders, exhibited significantly improved properties for the evaporation of water and overheating of the steam.
© 2004 Elsevier B.V. All rights reserved.

Keywords: Heat transfer; Microchannels; Micro-evaporator

1. Introduction

Electrically powered micro-heat exchangers [1] are devices combining arrays of microfabricated channels with conventionally fabricated electrical (resistive) heater elements in close proximity. Such devices allow a very efficient transfer of electrical power into thermal power, heating up and eventually evaporating a medium (here, water) flowing in the microchannels.

The behaviour of electrically powered micro-heat exchangers in the single phase regime, i.e. in the absence of evaporation, has been successfully simulated by CFD methods [2]. It has also been shown that more complex geometries of the microchannels can lead to increased efficiency of such devices [3]. For heat transfer in the presence of evaporation, simulation tools are under development [4]. It should, however, be noted that devices intended for laboratory or production purposes, characterised by a throughput of the order of kilograms per hour at a pressure drop of several hundred kPa, will necessarily have to contain a large number of microchannels (possibly hundreds or even thousands), while most investigations on evaporation in microchannels [5] or more generally on two-phase flow in microchannels [6] reported hitherto concentrate on single channels or small arrays of channels. The lack of understanding the two phase (liquid/steam) flow behaviour in microchannels and large arrays of microchannels is an obstacle towards the widespread use of electrically powered micro-heat exchangers as compact evaporators.

Experimental explorations of the device properties as presented in the following are necessary for a number of reasons. First, the experiments are to produce data against which simulation tools can be validated, especially in the two-phase regime. Second, simulations do not always cover all aspects of the environment, like heat losses via surfaces and tubing that are becoming more important at low throughputs. Third, assumptions about the spatial and temporal symmetry of the fluid flow as well as temperature and pressure fields in the devices have to be made in the setup of models for simulations, while the measurable device properties will be more or less sensitive to the degree of these symmetries. Measurements on the performance of the devices under realistic operating conditions have, therefore, not yet be obsoleted by the advances in simulation techniques. In addition, the unique properties of microstructure devices make them useful for some applications in chemical engineering even if these properties are not yet readily accessible by simulation methods.

Another consequence of the partial lack of simulation tools is that there is still room for the optimisation of devices by trial-and-error methods. This is especially true for electrically powered micro-evaporators, and in the following, a device designed intuitively for the purpose of

☆ Dedicated to Prof. G. Emig on the occasion of his 65th birthday.

* Corresponding author. Fax: +49-7247-82-3186.
E-mail address: torsten.henning@imvt.fzk.de (T. Henning).

1385-8947/$ – see front matter © 2004 Elsevier B.V. All rights reserved.
doi:10.1016/j.cej.2003.10.020

Nomenclature

A	microchannel cross-section area
c_p	specific heat capacity at p = const.
d_h	hydraulic diameter
h	microchannel depth
l	microchannel length
$\dot{m}$	mass flow rate
p	pressure
P_{el}	electrical power
P_{th}	thermal power
R_h	heater resistance
t	time
T	temperature (absolute)
$\{T_{cartr}\}$	heater cartridge temperatures
U_h	heater voltage, effective
$\bar{v}$	mean fluid velocity
$\dot{V}$	volume flow rate
w	microchannel width
X_{in}	X at water inlet
X_{out}	X at water/steam outlet
ΔX	difference of X between inlet and outlet

Greek symbol

η	power conversion efficiency
η'	viscosity

micro-evaporation, but without the guidance of simulation, will be compared to two devices whose design was subject to (single phase) CFD simulation prior to construction.

2. Devices

In this report, we focus on three devices which are shown in Fig. 1 and whose parameters are detailed in Table 1. All three devices were made in-house at Forschungszentrum Karlsruhe. The device with number 792-K-5.2 is a "standard" channel device consisting of six microstructured channel foils, each comprising 103 mechanically micromachined channels 54 mm long, 200 μm wide and 100 μm deep. These foils were stacked alternatingly with three metal blocks equipped with receptacle holes for electrical heater cartridges and two cover plates. Two microstructure foils were placed between any two heater blocks and one microstructure foil between the outermost heater blocks and the cover plates. The stack was joined by electron beam welding and fitted with adapters.

The "short" channel device with number 1123-K-5.2 differs from the standard device in the channel length, which had been reduced to 25.8 mm, and in the number of heaters (two per block instead of five). The third device has the same stack dimensions as the standard device, but instead of straight channels, each of the six microstructure foils contains 77 channels, each 300 μm wide and wet chemically etched to a depth of 100 μm, following a sinusoidal path. This third device with number 1116-B-5.0 is labelled as the "wavy" channel device. Scanning electron micrographs of the two types of channels are compared in Fig. 2.

The last column of Table 1 gives the hydraulic diameter of an equivalent device with the same number of channels of the same length, but with channels of circular cross-section. It was determined from the first order term in the measured pressure drop Δp of nitrogen at room temperature against flow rate $\dot{V}$, $\lim_{\dot{V}\to 0} \mathrm{d}(\Delta p)/\mathrm{d}\dot{V}$, analytically solving

$$\Delta p = \frac{32\eta' l \bar{v}}{d_h^2}, \tag{1}$$

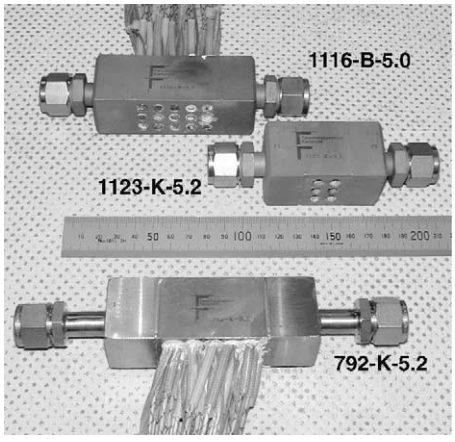

Fig. 1. Photograph of the devices. Two of the devices are loaded with fifteen heater cartridges each, and each heater cartridge is equipped with a thermocouple.

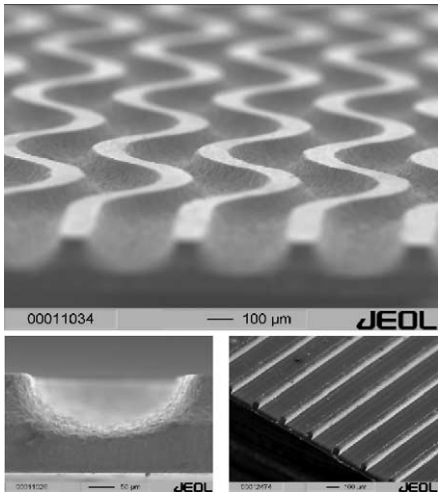

Fig. 2. Scanning electron micrographs of microstructure (channel) foils. Top: "wavy" channels following a sinusoidal path. The distance of the walls perpendicular to the direction of view in this image is constant, so that the cross-section perpendicular to the direction of flow has slight constrictions at the inclination points of the sine curves. Bottom left: cross-section detail of a wavy channel, made by wet chemical etching. Bottom right: mechanically micromachined channel foil, as used in the two straight channel devices.

Table 1
Characteristic parameters of the devices under test. d_h is the hydraulic diameter calculated from the pressure loss of gaseous nitrogen at low flow rates, assuming a circular channel cross-section

Serial number	Number of		Channel parameters				
	Channels	Cartridges	Cross-section	Length (mm)	Micro-fabricated	Layout	d_h (μm)
792-K-5.2	6 × 103	5 × 3	100 μm × 200 μm	54	Micro-machined	Straight	153
1123-K-5.2	6 × 103	2 × 3	100 μm × 200 μm	25.8	Micro-machined	Straight	149
1116-B-5.0	6 × 77	5 × 3	$w = 300$ μm, $h = 100$ μm	57.1	Etching	Wavy	125

where η' is the viscosity of nitrogen, l the channel length and $\bar{v}$ the average velocity of the gas, under the assumption that the cross-section is

$$A = \frac{\pi}{4} d_h^2. \quad (2)$$

The devices were heated by commercially available heater cartridges with a diameter of 0.25 in. and a length of 1.375 in., each providing a power of up to 225 W (at 230 V effective voltage).

3. Experimental procedures

Characteristics of the devices under test were measured in an automated computerised setup at constant power conditions. The sets of three heater cartridges each located at the same distance from in- and outlet were coupled together in parallel and supplied with a constant AC voltage, such that each of these (2–5) sets of cartridges dissipated the same amount of electrical power.

The water temperatures at in- and outlet were measured with type K (NiCr/Ni) thermocouples located inside the inlet adapter volume and in the connector behind the outlet adapter volume. In addition, temperatures inside the heater cartridges were measured by means of integrated type K thermocouples. These thermocouples were located on the inside of the heater cartridge steel skin at half the length of the cartridges. Their angular position at the cartridge circumference was unknown.

At each combination of fixed water throughput and (total) electrical power, these two parameters were kept fixed for a certain time, typically 1–5 min. The electrical power was then increased or decreased by a certain amount for the next measurement cycle. For each parameter combination, the temperature data during the last 30 s (corresponding to about 15–25 measurements of each value of the various temperatures) were evaluated for further analysis. The electrical power was increased until the output temperature of 373 K had been reached, or, in the case of evaporation experiments, until the first two of 15 heater cartridges had reached a temperature of 593 K. This temperature range was chosen in order not to risk rapid deterioration of the heater cartridges. Once the maximum pre-set temperature had been reached, the electrical power was decreased stepwise along the same values as before and measurements were continued. A waiting period too short to reach the steady state at any parameter combination would thus show up as a hysteresis when the corresponding quantity is plotted against the electrical power applied.

The devices were not equipped with any thermal insulation. The water supply temperature was between 282 and 294 K. With increasing heater power and at low flow rates, the inlet temperature T_{in} would rise above the supply temperature due to conductive and convective heat transfer against the direction of flow. To ensure uniform conditions for the three devices, they were always mounted vertically, with the water being pumped upwards.

4. Results and discussion

4.1. Thermal conversion efficiency

The thermal conversion efficiency η was calculated as the ratio of the thermal power P_{th}, needed to raise the temperature of water from T_{in} to T_{out}, to the electrical power applied P_{el},

$$\eta = \frac{P_{th}}{P_{el}} = \frac{\Delta T \dot{m} \langle c_p \rangle R_h}{U_h^2}, \quad (3)$$

where R_h is the resistance of the heater cartridges, U_h the effective voltage (true RMS) applied to them, and $\dot{m}$ the mass flow rate. The mean heat capacity $\langle c_p \rangle = (1/\Delta T) \int_{T_{in}}^{T_{out}} c_p(T)\, dT$ of water at a pressure around 10^5 Pa was calculated from tabulated values for c_p [7].

Eq. (3) is valid for the temperature range below the boiling point of water. In this range, the above-mentioned temperature increase of the water at the inlet due to heat flowing against the direction of the water flow could be neglected. Fig. 3 shows η as a function of P_{el} for an inlet flow at room temperature.

Several observations are immediately obvious. The device with shorter channels has a higher efficiency than the standard device for lower flow rates. At higher flow rates, the device with standard channels quickly reaches a plateau at an efficiency above 90% with increasing power. The efficiencies of the short channel device and of the wavy channel device drop stronger towards low power values than the efficiency of the standard channel device, especially for the higher flow rates. In general, the efficiency versus power plot

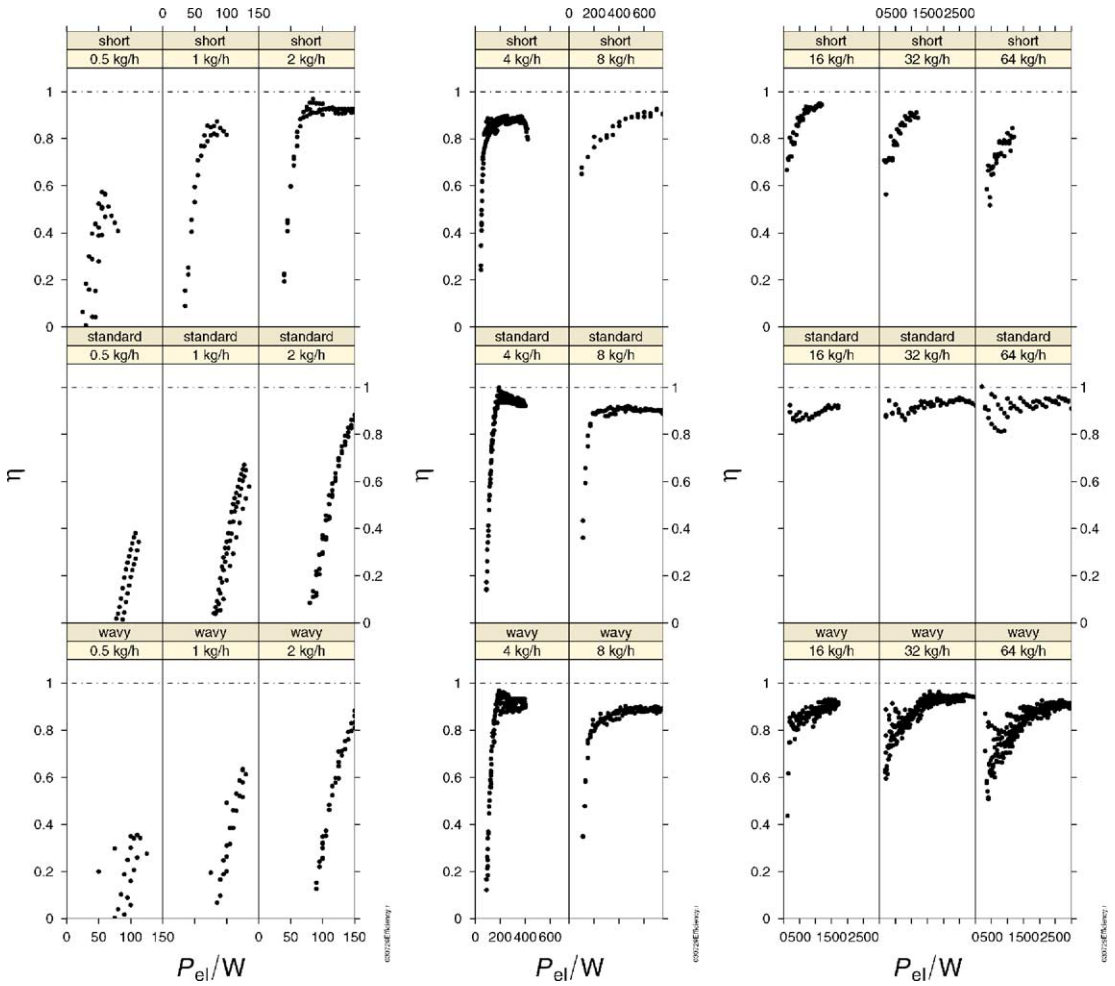

Fig. 3. Thermal conversion efficiency η for the three devices, measured at eight different flow rates, and plotted against the electrical power applied P_{el}. The label "standard" stands for the device with 54 mm long straight channels, "short" for the 25.8 mm channel device and "wavy" for the device with channels following a sinusoidal path in a 54 mm long block.

of the wavy channel device is more similar to that of the standard channel device for lower throughputs and more similar to that of the short channel device for higher throughputs.

The increased efficiency of the short channel device for lower throughputs points to heat loss via the side faces of the device as an important factor in the total heat loss at very low throughputs. This heat loss becomes less important at higher powers, when losses through the tubing and via the water against the direction of flow (raising T_{in} and thus reducing η as defined above) are dominating. The standard channel device is more effective than the short channel device at these higher powers, presumably since the distance of the centres of the microchannels from their inlets is larger. A reduced heat loss in backward direction is therefore to be expected for the standard device compared to the short channel device, but a quantitative description will require simulation calculations taking the environment into account. In addition, experiments could be done with improved thermal insulation at the various parts of the setup, possibly allowing to focus on individual heat loss paths. The similarity between the standard channel device and the wavy channel device in their heat transfer efficiencies is to be expected since the channels are quite similar in their hydraulic properties under single phase conditions and under laminar flow, and the difference in length due to the meandering is small (below 6%).

4.2. Wall excess temperature

Applying electrically powered micro-heat exchangers to heat up any fluid that may undergo chemical reactions, especially undesired side reactions or deterioration, at temperatures above the target outlet temperature, it becomes important to know the maximum temperature that the fluid may be exposed to during its passage through the microchannels. The excess of the maximum wall temperature above the outlet temperature is a property that is especially sensitive to the perfectness of the device symmetry and, therefore, hard to predict.

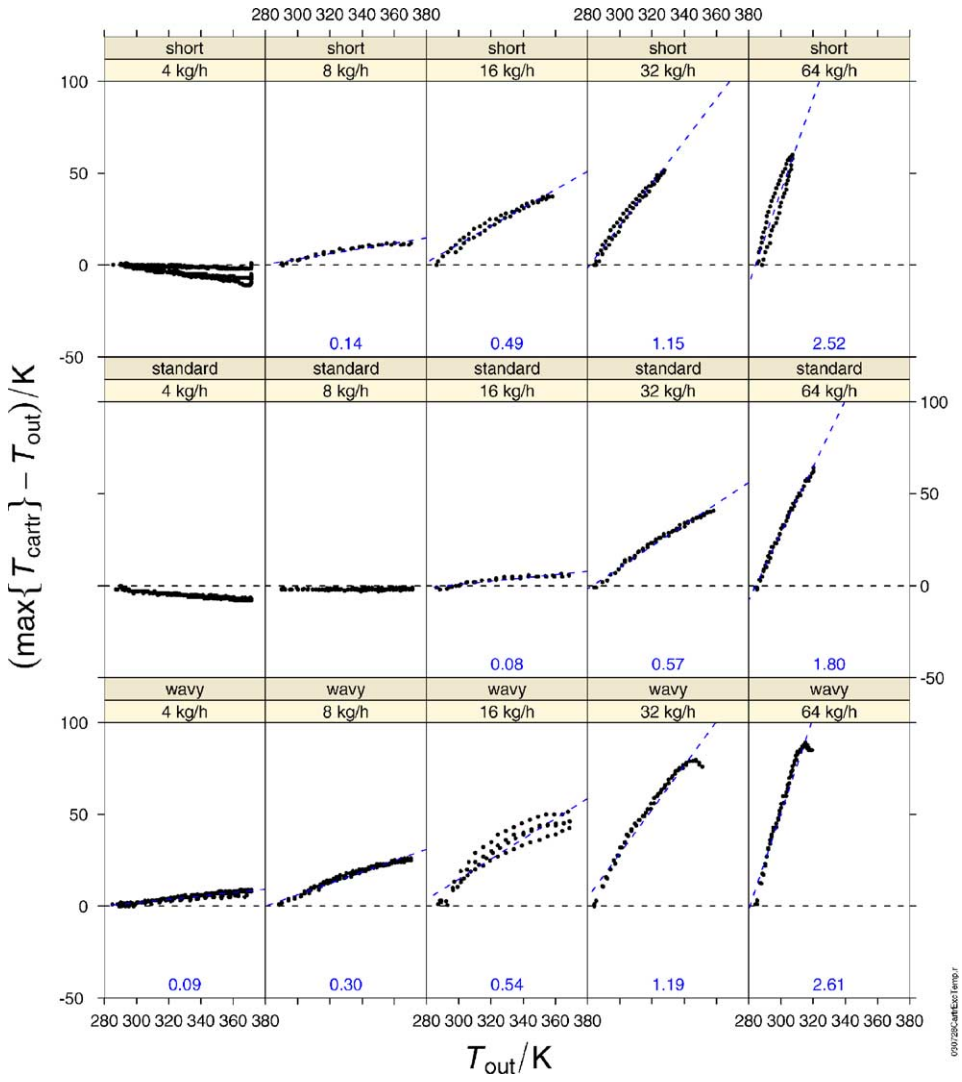

Fig. 4. Wall excess temperature: difference between the temperature of the hottest heater cartridge max{T_{cartr}} and the water temperature at the outlet T_{out}, as a function of T_{out}. Devices are labelled as in Fig. 3. The figure at the bottom of some panels is the slope of the dashed line, showing the result of a linear least-squares fit to the maximum temperature difference data.

While the small number of micro-heat exchanger devices characterised so far necessarily limits the statistical significance of investigations, nevertheless interesting patterns can be found in the data already available.

Fig. 4 shows how the maximum cartridge temperature varies with the output temperature in the range below the boiling point. The heater cartridge temperatures are the best measure accessible of the real wall temperatures that the fluid inside the device is exposed to. The maximum heater cartridge temperatures are of course to a certain extent sensitive to deviant behaviour of individual heater cartridges or microchannel layers. Indicators of such a deviant behaviour were, however, not observed in the devices considered here. Some other devices showed significant asymmetries between layers that may be related to variations in the micro-fabrication process chain. In such devices, presumably originating from a narrower portion of the microchannel array, the formation of hot spots was observed in the evaporation regime. Thermography of the device surface then sometimes indicated significantly colder water passing through the other channels, while the channels around the hot spot obviously suffered from the well-known problem of “vapour clogging”. None of the three devices compared here, however, showed such a hot spot.

For all three devices in Fig. 4, the outlet temperature is determined by the hottest heater cartridge at low flow rates. While for the short channel and the wavy channel devices this low flow rate range already ends somewhere below 8 kg/h, in the standard channel device the outlet temperature still follows the maximum heater temperature at twice this throughput. Overall, the standard channel device is obviously the best choice for heating up sensitive liquids at moderate and higher flow rates.

The wavy channel device, however, shows an interesting difference in its characteristics at high flow rates compared to the straight channel devices. While for the latter, the wall excess temperature increases approximately linearly with the outlet temperature, the slope of the corresponding curve for the wavy channel device is decreasing. As the temperature approaches the boiling temperature, the mean wall temperature excess tends towards zero for a flow rate around 16 kg/h, tends to level off at twice this rate, and to at least slow down at even higher flows. This behaviour made it seem worthwhile to investigate the wavy channel device at higher temperatures, namely in the evaporation regime.

4.3. Evaporation of water

For a small flow rate of 0.5 kg/h, both the device with (standard) straight channels and the wavy channel device performed well at the evaporation of water and the overheating of steam. Fig. 5 shows the experimental data. It should be noted that the power conversion efficiency of both devices as evaporators is much larger at this small flow rate than their efficiency in the temperature range below the onset of boiling.

The wavy channel device showed a narrower distribution of heater cartridge temperatures than the straight channel device. For a sound statistical analysis, however, more devices will have to be manufactured and characterised. Also, the effect of uncertainties in the channel dimensions and surface properties, as well as variations introduced by processing steps after the microchannel structuring, will have to be explored.

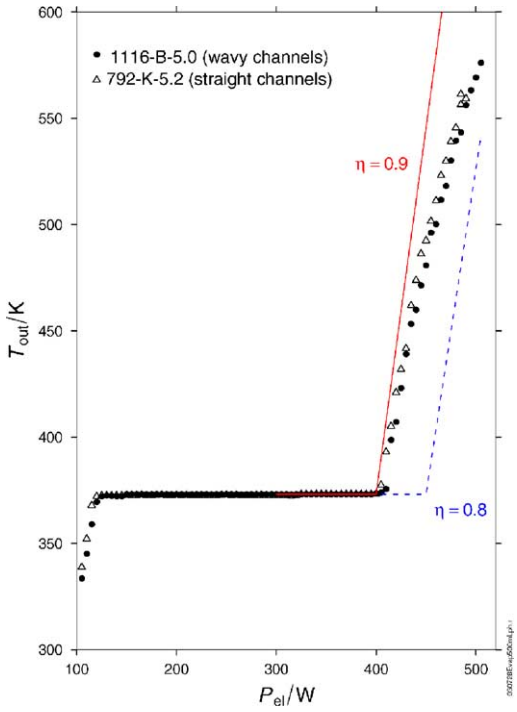

Fig. 5. Evaporation of water and overheating of steam at 0.5 kg/h: outlet temperature against electrical power applied. In the overheating region, the power was increased by 5 W every 240 s. Shown are the averaged data of the last 30 s of every step. The experiments were aborted when at least two of the 15 heater cartridges had exceeded 573 K. Any difference between the two devices is non-significant. The dashed and solid lines mark the output temperature of a hypothetical device with the power conversion efficiencies 0.8 and 0.9, respectively, over the entire temperature range.

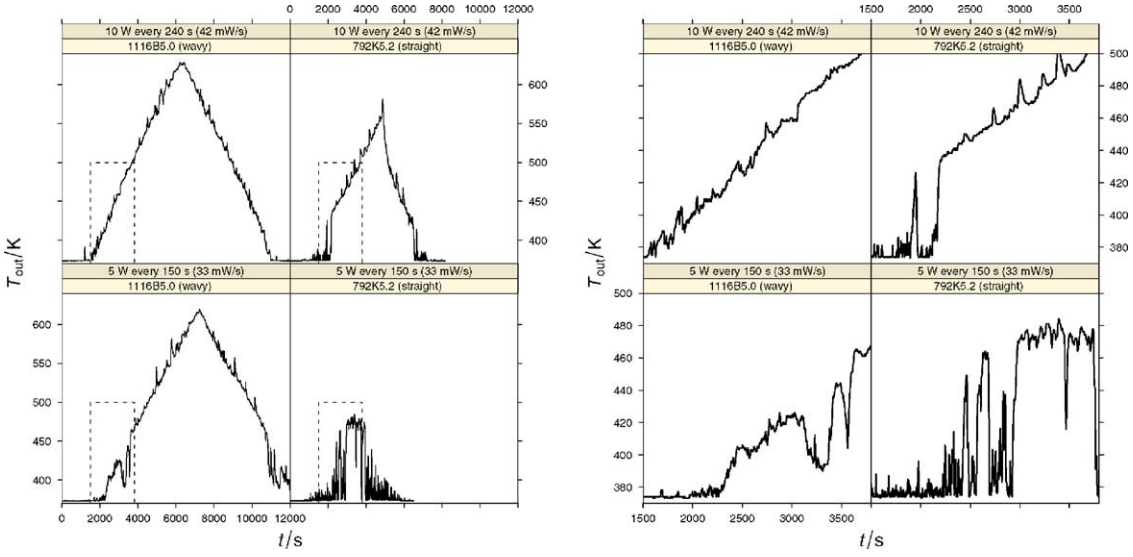

Fig. 6. Attempts at the overheating of 1 kg/h steam: outlet temperature against time. The devices had been pre-heated at 750 W electrical power for ten minutes, then the clock was started and the power was increased stepwise as indicated in the upper strip of each panel. The direction of power ramping was reversed when at least two of the 15 heater cartridges had exceeded 573 K (left panels). Right panels: detail magnification, zooming in on the transition between the saturation region and the steam overheating region. Device 1116-B-5.0 with the wavy channels showed significantly more stable behaviour than the straight channel device 792-K-5.2.

While the transition from the saturation region to the overheating region was rather smooth for both devices at a flow rate of 0.5 kg/h, differences between the devices became very obvious when the flow rate was doubled to 1 kg/h. Fig. 6 shows traces of the outlet temperature plotted against time, recorded while slowly stepping up the electrical power applied.

The straight channel device exhibited a rather unstable behaviour. It was not possible to just slightly overheat the steam with this device. The outlet temperature had to exceed 440 K in order to be relatively stable with time. Between 373 and 440 K, the straight channel device produced pulses of overheated steam alternating with pulses of fluid at the saturation temperature. Steam could, however, be overheated to just a few Kelvin above 373 K in the wavy channel device (at an average power ramp rate of 42 mW/s) with a good stability.

At a lower power ramp rate, both devices performed worse with regard to stability. As can be seen in the lower left panels of Fig. 6, the wavy channel device was reasonably stable at an outlet temperature above 440 K, while the straight channel device did not become stable before the power ramping had to be aborted due to excessive cartridge heating.

The wavy channel obviously assists in achieving total evaporation by separating remaining liquid droplets in every turn, driving them towards the hot channel surfaces by centrifugal forces, while the presence of a direct line of sight between inlet and outlet of the straight channels may allow vapour to accelerate liquid droplets drastically, shortening the contact time, or to separate the liquid from the walls. It is difficult, however, to separate the effects that the curvedness of the channels on one hand and the variation of the cross-section perpendicular to the flow on the other hand may have. At least two new types of devices will have to be manufactured to allow a valid generalisation of results here. The details of the evaporation process in these narrow confines and at the relatively high temperatures and power densities involved here remain to be investigated [8,9].

5. Conclusions

veral electrically powered micro-heat exchangers made at Forschungszentrum Karlsruhe were characterised for their power conversion efficiency, the excess of the wall temperatures above the outlet temperatures. First experiments on the stability of evaporation and steam overheating were made. Different designs showed advantages (and shortcomings) in different ranges of throughput and power or temperature under steady state conditions. Under realistic operating conditions, especially at low flow rates, heat loss is non-negligible, and future simulation work as well as experimental work needs to take this into account.

Data on the variation of the properties listed above with throughput and electrical power should now available should allow to assess whether these devices are suitable for a specific application, provided the fluid does not differ too much from water in its thermal properties. The characterisation will have to be extended to the dynamic behaviour of the devices, both to the response to sudden changes as well as to the behaviour in a control loop.

For microevaporator applications, one design employing channels following a sinusoidal path showed promising behaviour, especially compared to a straight channel device. This improvement can be intuitively understood, but the evaporation process in arrays of microchannels is a very complex process, posing challenges for both experiment and simulation. First simulation results for evaporation in straight channels with an improved porous medium approach are available and appear promising.

The dynamic characteristics of microchannel devices will be even more important for microevaporator applications than for heater applications, and future experiments need to provide both temporal and spatial resolution instead of only integral measurements. Especially, high speed microimaging is expected to be a useful tool in the trial-and-error method optimisation of microevaporator foils.

References

[1] K. Schubert, J. Brandner, M. Fichtner, G. Linder, U. Schygulla, A. Wenka, Microstructure devices for applications in thermal and chemical process engineering, Microscale Thermophys. Eng. 5 (2001) 17–39.
[2] A. Wenka, J. Brandner, K. Schubert, A computer-based simulation of the thermal processes in an electrically powered micro-heat exchanger, in: Proceedings of the Sixth International Conference on Microreaction Technology, AIChE Spring Meeting, New Orleans, LA, USA, March 10–14, 2002, pp. 345–350. ISBN 0-8169-9779-9.
[3] J.J. Brandner, M. Fichtner, U. Schygulla, K. Schubert, Improving the efficiency of micro-heat exchangers and reactors, in: R. Irven (Ed.), Fourth International Conference on Microreaction Technology, IMRET 4, AIChE Spring National Meeting, Atlanta, GA, March 5–9, 2000, Topical Conference Proceedings, New York, NY, 2000, pp. 244–249.
[4] U. Imke, Porous media simplified simulation of single- and two-phase flow heat transfer in micro-channel heat exchangers, in: Proceedings of the Seventh International Conference on Microreaction Technology, IMRET 7, CH-Lausanne, September 7–10, 2003, Book of Abstracts, DECHEMA, DE-Frankfurt, 2003, pp. 64–66 (published in summary form only).
[5] S.G. Kandlikar, Fundamental issues related to flow boiling in minichannels and microchannels, Exp. Therm. Fluid Sci. 26 (2002) 389–407.
[6] A. Serizawa, Z. Feng, Z. Kawara, Two-phase flow in microchannels, Exp. Therm. Fluid Sci. 26 (2002) 703–714.
[7] VDI-Wärmeatlas: Berechnungsblätter für den Wärmeübergang, vol. 8. Auflage, 1997.
[8] X.F. Peng, H.Y. Hu, B.X. Wang, Boiling nucleation during liquid flow in microchannels, Int. J. Heat Mass Transf. 41 (1) (1998) 101–106.
[9] X. Peng, H. Hu, B. Wang, Bubble formation of liquid boiling in microchannels, Sci. China Ser. E 41 (4) (1998) 404–410.